

# Interfacial mixing in heteroepitaxial growth

Boris Bierwald<sup>1</sup>, Michael von den Driesch<sup>1</sup>, Zéno Farkas<sup>1</sup>, Sang Bub Lee<sup>1,2</sup>, Dietrich E. Wolf<sup>1</sup>

<sup>1</sup> *Institut für Physik, Universität Duisburg-Essen, D-47048 Duisburg, Germany*

<sup>2</sup> *Department of Physics, Kyungpook National University, Taegu, 702-701 Korea*

We investigate the growth of a film of some element  $B$  on a substrate made of another substance  $A$  in a model of molecular beam epitaxy. A vertical exchange mechanism allows the  $A$ -atoms to stay on the growing surface with a certain probability. Using kinetic Monte Carlo simulations as well as scaling arguments, the incorporation of the  $A$ 's into the growing  $B$ -layer is investigated. Moreover we develop a rate equation theory for this process. In the limit of perfect layer-by-layer growth, the density of  $A$ -atoms decays in the  $B$ -film like (distance from the interface)<sup>-2</sup>. The power law is cut off exponentially at a characteristic thickness of the interdiffusion zone that depends on the rate of exchange of a  $B$ -adatom with an  $A$ -atom in the surface and on the system size. Kinetic roughening changes the exponents. Then the thickness of the interdiffusion zone is determined by the diffusion length.

PACS numbers: 68.35.Fx, 81.15.Aa, 81.15.Kk

## I. INTRODUCTION

Heterolayers, where e.g. ferromagnets are in contact with antiferromagnets, semiconductors or superconductors, give rise to new ordering and transport phenomena, which depend crucially on the interfacial structure. Examples for such ordering phenomena are the exchange bias [1], or the cryptomagnetism [2]. Electronic transport through a ferromagnetic-nonmagnetic-ferromagnetic sandwich (“spin valve” geometry) gives rise to the giant magneto-resistance [3,4]. Another example is the recently predicted possibility to enhance or reduce a Josephson current magnetically by replacing the tunnel barrier of a Josephson junction by a ferromagnetic-insulating-ferromagnetic sandwich [5]. These phenomena belong to the growing field of spintronics [6], where the spin degree of freedom is used for electronic signal processing. Interfacial mixing affects all of them [7]. For example, it leads to spin scattering disturbing the spin dependent transport properties.

Therefore it is important to be able to control the various physical processes that may spoil well defined interfaces. Some of them proceed after growth such as bulk interdiffusion or chemical interface reactions like silicide formation. However, there are also important processes taking place exclusively at the surface: For example the substrate may partially behave like a surfactant, when one grows a different material on it. It is this latter mechanism which we investigate in this paper. The questions we want to answer concern the asymptotic concentration profile, the width of the interdiffusion zone and possible correlations among the substrate impurities within the growing layer.

Specifically we consider growing some material  $B$  on a substrate  $A$ . Obviously the interfacial mixing requires that some substrate ( $A$ -) atoms get replaced by  $B$ -atoms and “float up” on the surface until they get incorporated into the growing film. There is ample experimental evidence that such a behaviour occurs in very different sys-

tems like Cr on Fe [8], AlAs on GaAs [9], Nb on Fe [10] or Au on Fe [11]. This process depends on several important parameters including the lattice mismatch and the interaction between the different atoms including magnetic contributions. In particular the explanation of any ordering of  $A$ - and  $B$ -atoms close to the interface would require a detailed investigation of these interactions [12].

The situation becomes considerably simpler, however, if one is interested in the physical properties further away from the interface. Then the concentration of  $A$ -atoms may be regarded as sufficiently low that their interaction as well as  $A$ - $B$ -ordering become unimportant. The focus on this region justifies our simplified model, in which the interdiffusion zone depends only on the deposition rate  $F$  of  $B$ -atoms, the diffusion constants  $D_A$  and  $D_B$  of the adatoms of type  $A$  or  $B$ , respectively, and the rate  $E$  for the exchange of  $B$ -adatoms with  $A$ -atoms. The limit  $E/D_B \rightarrow \infty$ , where a  $B$ -adatom exchanges with the first  $A$ -atom it encounters, would be realized, if the  $B$ -adatoms diffuse by an exchange mechanism [13], while the  $A$ -adatoms diffuse by hopping. In the present paper we simplify the model even further by assuming that both kinds of atoms diffuse equally fast on the surface,  $D_A = D_B = D$ , with a diffusion constant independent of the surface composition.

Apart from the exchange there is a second crucial ingredient in the model: The  $A$ -atoms behave only *partially* as a surfactant in the sense that they can be overgrown by island edges. By contrast a perfect surfactant atom should “float up” also in front of an advancing island edge.

Naively one would expect an exponential decay of the density profile of  $A$ -atoms far from the interface. It is the main result of this investigation that this is not always the case: The incorporation of  $A$ -atoms is much slower, giving rise to a power law decay of the concentration profile in the limit of perfect layer-by-layer growth,  $D/F \rightarrow \infty$ . In this case the width of the interdiffusion zone diverges, provided there are no finite size effects. By

contrast, we shall show that for finite  $D/F$  the width of the interdiffusion zone is no longer infinite, but a power law of  $D/F$ .

This paper is organized as follows. In the next section we are going to define a simple solid-on-solid (SOS) model for epitaxial growth of a  $B$ -layer on an  $A$ -substrate, which allows for the irreversible exchange of  $B$ -atoms with  $A$ 's at the surface. In this model the  $A$ -atoms on the surface turn out to cluster in a time-periodic self-organized way, which is explained in Sec.III. The next three sections, Sec.IV – VI, are devoted to the limit  $D/F \rightarrow \infty$ . First, in Sec.IV, we present a simple mean field argument leading to the prediction, that the concentration of  $A$ 's decays algebraically in the  $B$ -layer. For a finite system size this power-law is cut off leading to a finite width  $H$  of the interdiffusion zone, which is discussed in Sec.V, where also a scaling ansatz for the surface concentration  $c_A$  is proposed. This scaling ansatz is confirmed by simulation results for one- and two-dimensional surfaces in Sec.VI. The remaining sections deal with interdiffusion for finite  $D/F$ . Sec.VII contains simulation results and scaling arguments, and in Sec.VIII a rate equation theory is developed for the interdiffusion problem. In the Appendix we describe a very efficient implementation of the simulation model for one-dimensional surfaces in the limit  $D/F \rightarrow \infty$ .

## II. THE MODEL

In order to model heteroepitaxial growth of a  $B$ -layer on an  $A$ -substrate including the interfacial mixing, we introduce a simple solid-on-solid (SOS) model, where the lattice mismatch and most interactions between the atoms are neglected. Moreover we describe the exchange mechanism of  $B$ -adatoms with  $A$ -atoms in the surface simply by a phenomenological constant exchange rate  $E$ , although it depends in reality on the system parameters as well as the local environment.

The model is defined on a simple cubic lattice by the following kinetic rules (cf. Fig. 1):

- (1) Starting from an initially flat substrate consisting of  $A$ -atoms,  $B$ -atoms are deposited at randomly selected sites on the surface with deposition rate  $F$ .
- (2) As long as they do not have a lateral neighbor, the  $B$ -atoms diffuse on the surface with diffusion constant  $D$ .
- (3) When such a  $B$ -atoms happens to sit on top of a  $A$ -atom, it can exchange vertically with rate  $E$  or continue to diffuse with rate  $D$ .
- (4) After an exchange, the  $B$ -atom stays irreversibly bound, whereas the  $A$ -atom diffuses on the surface with diffusion constant  $D$ .
- (5) There is *no* back exchange, when a  $A$ -atom sits on top of a  $B$ -atom.
- (6) When two adatoms, regardless of their type, meet, they form a stable non-moving nucleation center of an island.

(7) When an adatom, regardless of its type, reaches a site adjacent to an island, it is irreversibly bound, increasing the size of the island.

(8) Both types of particles can diffuse down across terrace edges without being hindered by an Ehrlich-Schwoebel barrier.

(9) There are no overhangs, i.e., we assume SOS growth.

(10) The exchange of a  $B$ -atom with an  $A$ -atom underneath is forbidden, if the  $B$ -atom is already part of an island, i.e., if it has a nearest neighbor at the same height. Hence  $A$ -atoms can be overgrown by island edges.

Measuring time in units of monolayers (ML) and lengths in units of the lattice constant  $a$ , this model is controlled by the two dimensionless parameters  $D/Fa^4$  and  $r_E \equiv a^2 E/D$ . (In the following we set  $a = 1$ .)

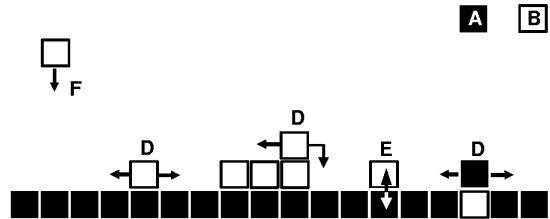


FIG. 1. The growth process of the model.  $B$ atoms are deposited with a deposition rate  $F$  onto the substrate. Adatoms diffuse on the surface and down to the binding site at an island edge with diffusion constant  $D$  irrespective of their type. In the top layer mobile  $B$ 's can exchange with  $A$ 's with an effective exchange rate  $E$ .

This model will be investigated for one- and two-dimensional ( $d = 1$  and  $d = 2$ ) surfaces in the following. Note that it reduces to the usual model for MBE growth (for a recent review see e.g. [14]), if one does not distinguish the two particle types. Therefore, the  $D/F$ -dependence of quantities like island density, adatom density, surface width, etc. are the same as usual. For general values of  $D/F$  and  $E/D$  we use kinetic Monte Carlo simulations [15,16] in order to investigate the model. However, for one-dimensional surfaces in the limit  $D/F \rightarrow \infty$  we implemented a much more efficient algorithm, which is described in the Appendix.

## III. CORRELATIONS OF THE A-ATOMS

One of the most intriguing qualitative properties of this model is the time-periodic self organization of  $A$ -clusters on the growing surface with a period of one monolayer. Fig.2 shows that the  $A$ -atoms (black) are first clustered around the nucleation sites of a new layer, but migrate towards the holes remaining in that layer, when the islands coalesce. Thus the characteristic distance between these clusters agrees with the typical distance between

the nucleation sites, the diffusion length

$$\ell_D \sim (D/F)^\gamma, \quad (1)$$

as long as layer-by-layer growth persists. This can be verified by examining the lateral correlations of  $A$ -atoms on the surface after deposition of  $t$  monolayers:

$$g(\vec{r}, t) = \frac{1}{L^d} \sum_{\vec{x}=1}^{L^d} \rho_A(\vec{x}, t) \rho_A(\vec{x} + \vec{r}, t) - c_A(t)^2, \quad (2)$$

where  $\rho_A(\vec{x})$  denotes, whether there is an  $A$ -atom at the surface at site  $\vec{x}$  [ $\rho_A(\vec{x}) = 1$ ] or not [ $\rho_A(\vec{x}) = 0$ ], and  $c_A(t)$  denotes the surface density of  $A$ -atoms.  $d$  is the dimension of the surface. In our simulations,  $d$  was 1 or 2. A data collapse of these correlation functions for different values of  $D/F$  is obtained, if the space coordinates are rescaled by  $\ell_D$  (see Fig. 3 for  $d = 1$ ), which shows that this is the characteristic distance between the  $A$ -clusters.

The mechanism of the periodic self organization can most clearly be seen in the limit  $r_E = E/D \rightarrow \infty$ , where every  $B$ -adatom exchanges with the first exchange partner  $A$  it encounters. When layer  $t$  is completed and layer  $t+1$  begins to grow, the first  $B$ -atoms deposited are likely to exchange with  $A$ -atoms from layer  $t$ . Hence the nuclei of islands in the new layer  $t+1$  will consist predominantly of  $A$ -atoms. As growth proceeds, the lower terrace (layer  $t$ ) gets depleted from exchange partners  $A$ , either because they are exchanged with freshly deposited  $B$ -adatoms or get overgrown by the islands. Then the core of the islands with a high concentration of  $A$ -atoms gets surrounded by mainly  $B$ -atoms (Fig. 2, left). However, as the island size increases, it becomes more and more likely that  $B$ -atoms are deposited on top of the islands, i.e. in layer  $t+2$ . These  $B$ -adatoms find many exchange partners at the core of the islands, which then become “washed out” and start decorating the island edges, because there are no Ehrlich-Schwoebel barriers in our model. Note that this edge decoration with  $A$ -atoms happens *without lateral exchange* of  $B$ - with  $A$ -atoms at the edges of the islands, in contrast to the situation studied in [17]. As a result, the interior of the islands gets cleared from  $A$ -atoms, which are collected in the holes of layer  $t+1$  which get filled last (Fig. 2, right). Then the process starts again: Layer  $t+2$  nucleates predominantly with  $A$ -atoms which were exchanged from layer  $t+1$ .

For finite  $r_E$  the mechanism is similar. However, for vicinal surfaces growing in step flow mode, the correlations among the  $A$ -atoms are different. Here, the terraces get cleared of  $A$ -atoms, which attach to the step edges. This decoration of advancing edges leads to a correlation pattern  $g(\vec{r}, t)$  with a spatial periodicity identical to the width of the terraces.

#### IV. THE SCALE FREE LIMIT

The limit of perfect layer-by-layer growth,  $D/F \rightarrow \infty$ , is particularly instructive. In this case, there is only one

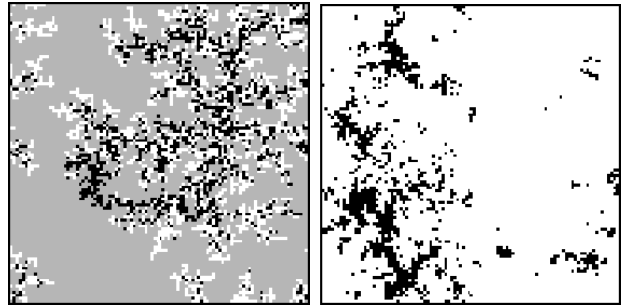


FIG. 2. Top view on the surface structure at  $t = 3.3$  ML (left) and  $t = 4.0$  ML (right).  $A$ -atoms are black,  $B$  atoms are height-encoded, where brighter means higher.  $D/F = 10^7$ ,  $E/D = 10^3$ ,  $L^2 = 100 \times 100$ .

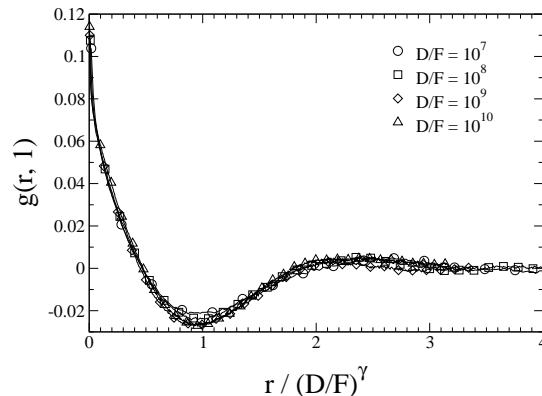


FIG. 3. Rescaled lateral  $A$ - $A$  correlation functions  $g(r, t)$  at  $t = 1$  for different  $D/F$  ( $d = 1$ ). The average distance between  $A$ -clusters scales with  $D/F$  like the distance of the nucleation sites,  $\ell_D$ .

island on the surface, nucleating at a random site. Afterwards at most one adatom can be found on the surface at a time. If we assume maximal exchange in addition, i.e. an exchange rate  $E$  much larger than both  $D$  and  $F$ ,  $r_E = E/D \rightarrow \infty$ , the model becomes parameter-free.  $A$ -atoms can be buried even in this limit, when they are overgrown by an island edge. However, the last  $A$ -atom will never get buried in this case. The nucleus of a new layer will always contain at least one of the remaining surface atoms of type  $A$  in the limit we focus on, because the first  $B$ -atom deposited after completion of a layer exchanges with an  $A$ -atom before the next  $B$ -atom gets deposited:  $c_A(t \rightarrow \infty) = L^{-d}$ . As this case is scale free, we expect that the concentration of  $A$ -atoms falls off like a power law into the growing  $B$ -film.

In order to get a first idea about the distribution of  $A$ -atoms in the growing  $B$ -film, it suffices to consider the concentration  $c_A(n)$  of  $A$ -atoms at the surface after the

deposition of  $n$  monolayers. During the growth of the next layer, a certain fraction  $(1 - q) \in [0, 1)$  of these  $A$ -atoms is transported to the next layer via vertical exchange:

$$c_A(n+1) = (1 - q)c_A(n). \quad (3)$$

If  $q$  was constant, this would imply an exponential decay  $c_A(n) \propto (1 - q)^n$ . In the present model, however, the probability  $q$  that an  $A$ -atom gets overgrown decreases with decreasing  $c_A(n)$ , resulting in a decay which is slower than exponential.

Qualitatively this can be understood in the following way: In the limit  $D/F \rightarrow \infty$  there is only one island on the surface. Moreover, any  $A$ -atom on the lower terrace gets transferred to the new layer as soon as it is reached by an adatom of type  $B$ , because  $r_E \rightarrow \infty$  is assumed, as well. Only  $A$ -atoms sufficiently close to the island have a chance to be overgrown by the island edge before being visited by a  $B$ -atom.

The island edge advances a characteristic distance  $\ell_{\text{cover}}$ , while the lower terrace gets depleted from  $A$ -atoms by exchange with adatoms of type  $B$ . For a one-dimensional surface of length  $L$  it is clear that  $\ell_{\text{cover}}$  is proportional to the number of  $A$ -atoms at the surface,  $c_A(n)L$ . Hence, the number of  $A$ -atoms with a chance to be overgrown is of the order of

$$\ell_{\text{cover}}c_A(n) \propto c_A(n)^2L. \quad (4)$$

This must be compared with  $qc_A(n)L$ , which shows that

$$q \propto c_A(n). \quad (5)$$

Inserting Eq.(5) into Eq.(3) leads to the difference equation

$$c_A(n+1) - c_A(n) \propto -c_A(n)^2 \quad (6)$$

implying the asymptotic power law

$$c_A(n) \sim 1/n \quad (7)$$

for the concentration of  $A$ -atoms at the surface.

The concentration profile of  $A$ -atoms inside the grown film is given by

$$\rho(n) = c_A(n) - c_A(n+1) \sim 1/n^2. \quad (8)$$

It is remarkable that for the mechanism discussed in this paper the width of the interdiffusion zone diverges logarithmically with the thickness  $T$  of the film:

$$\sum_{n=1}^{T-1} \rho(n)n + c_A(T)T \sim \ln T. \quad (9)$$

Nevertheless, the interface can be localized precisely, because  $B$ -atoms do not occur below layer  $n = 0$  due to the absence of bulk diffusion in this model. Below we show that these power laws are confirmed by simulations.

The argument leading to Eq.(5) ignores that the  $A$ -atoms at the surface are clustered, as shown in Fig.2, and was made plausible only for a one-dimensional surface. However, it can be refined such that it takes these spacial correlations into account and applies also for two-dimensional surfaces. For  $D/F \rightarrow \infty$ , we can imagine that there is only one cluster of size  $c_A(n)L^d$  on the surface, when the new layer nucleates. The important point is that the nucleation happens anywhere on the surface with equal probability  $1/L^d$  in this case. However, only if the nucleation site is within an area of about the size  $2^d c_A(n)L^d$  centered at the middle of the cluster, there is a chance that some  $A$ -atoms get overgrown. In other words, only a fraction of nucleation sites  $\propto c_A(n)$  leads to overgrowth. The average number of  $A$ -atoms overgrown in such a case is proportional to the cluster size. Hence on average a fraction  $q$  of  $A$ -atoms is overgrown which is proportional to the fraction of nucleation sites leading to overgrowth, i.e. this refined argument gives  $q \propto c_A(n)$  as in Eq.(5).

## V. THE WIDTH OF THE INTERDIFFUSION ZONE FOR $D/F \rightarrow \infty$

In the previous section we predicted that the width of the interdiffusion zone diverges in the scale free limit, where  $D/F \rightarrow \infty$  and  $r_E \rightarrow \infty$ . In this section we predict, that for finite  $r_E$  the power law Eq.(7) is only valid, if the system is infinitely large. For finite system size the power law is exponentially cut off at a characteristic width of the interdiffusion zone.

After the completion of several monolayers on a substrate of linear size  $L$  the number of substrate atoms at the surface is  $c_A L^d$ . The  $A$ -atoms are concentrated in a cluster, which we assume to be compact, hence of diameter  $\propto c_A^{1/d} L$ . This assumption is justified even for  $d = 2$ , where the islands initially are fractal, because the  $A$ -cluster occupies the sites which were filled *last* in the uppermost monolayer. These sites do not form a fractal.

Now we imagine the surface to be coarse grained on the scale of the cluster diameter so that exactly one cell contains the  $A$ -cluster. The typical residence time of an adatom in such a cell is

$$\Delta t = \frac{(c_A^{1/d} L)^2}{D}. \quad (10)$$

A  $B$ -adatom which enters the cell containing the  $A$ -cluster will almost certainly be replaced by an exchange partner  $A$  within the residence time, if

$$E\Delta t = r_E(c_A^{1/d} L)^2 \gg 1 \quad (11)$$

(exchange dominates). For  $E\Delta t \ll 1$  the adatom changes from type  $B$  into type  $A$  only with probability  $E\Delta t$  (overgrowth dominates).

It is plausible to assume that the power law belongs to the exchange dominated slow decay of  $c_A$  while the

exponential cut off indicates the much faster decay when overgrowth dominates. Thus the width  $H$  of the interdiffusion zone should be reached, when  $c_A$  becomes so small that exchange is no longer guaranteed, i.e. when  $E\Delta t$  drops below 1. Inserting  $c_A \approx 1/t = 1/H$  into Eq.(11) one obtains

$$H \approx (\sqrt{r_E L})^d. \quad (12)$$

However, as  $c_A$  cannot become smaller than  $L^{-d}$ , this estimate is only valid for  $r_E < 1$ , while  $H \approx L^d$  for  $r_E > 1$ . This is our prediction for the width of the interdiffusion zone in the limit  $D/F \rightarrow \infty$ . Note that in this limit the cutoff of the power law is a finite size effect: For  $L \rightarrow \infty$  the power law extends to infinity.

Based on the results of this and the previous paragraph we can conjecture the following scaling form for the surface concentration of  $A$ 's :

$$c_A(t, L; r_E) - c_A(t \rightarrow \infty) = \frac{1}{H} f\left(\frac{t}{H}\right) \quad (13)$$

where according to Eq.(7)

$$f(\tau) \sim 1/\tau \quad \text{for } \tau \ll 1. \quad (14)$$

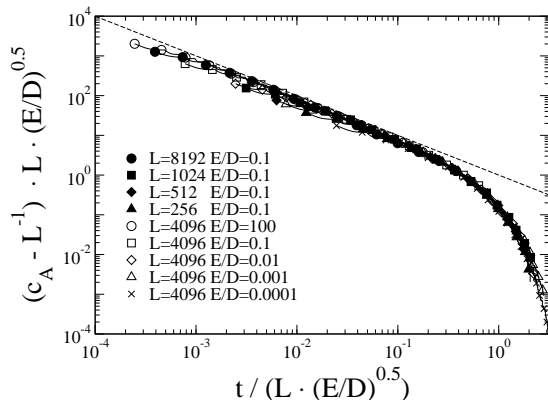


FIG. 4. Scaling of  $c_A(t)$  with  $L$  and  $E/D$  in  $d = 1$  for  $D/F \rightarrow \infty$ . Full symbols mark four curves for  $E/D = 0.1$  and  $L$  between 256 and 8192. Open symbols mark five curves for  $L = 4096$  and  $E/D$  between  $10^{-4}$  and 100. A data collapse of all 9 curves is reached by scaling in accordance with Eq.(13) and Eq.(12). The data for  $E/D = 100$  were rescaled differently: Here,  $c_A L - 1$  is plotted vs.  $t/L$ , as if  $E/D$  was 1 instead of 100. This shows, that  $H$  becomes independent of  $E/D$  for  $E/D > 1$  as explained after Eq.(12). The dashed line has slope -1 in agreement with Eq.(14).

## VI. NUMERICAL RESULTS FOR $D/F \rightarrow \infty$

In order to check the predictions of Secs. IV and V, we simulated the model described in Sec.II for  $D/F \rightarrow \infty$

and varied the values of  $r_E$  and system size  $L$  for one- and two-dimensional surfaces. For the case  $d = 1$  we used the algorithm described in the appendix, while kinetic Monte-Carlo simulations were done for  $d = 2$ .

Fig. 4 (for  $d = 1$ ) and Figures 5, 6 (for  $d = 2$ ) show the concentration  $c_A$  of  $A$ -atoms at the surface as a function of deposition time  $t$  (in monolayers of  $B$ -atoms). All curves are averages over 200 - 400 independent runs. Both for  $d = 1$  and  $d = 2$  the exponent of the power law decay was found to be consistent with the value -1 derived in section IV.

As shown in Fig. 4, the predicted relations Eq.(12) and Eq.(13) lead to the expected data collapse for the one dimensional surface. The results in two dimensions are not as clear. In this case, we obtain the best data collapse with

$$H \propto L^{1.93} \cdot r_E^{1.2}, \quad (15)$$

as shown in the Figures 5 and 6, whereas our predicted exponents (2 and 1, respectively, see Eq.(12)) were about 4% and 20% different. In fact the  $A$ -clusters are not as compact as assumed in the simple argument of Sec.V (see Fig.2).

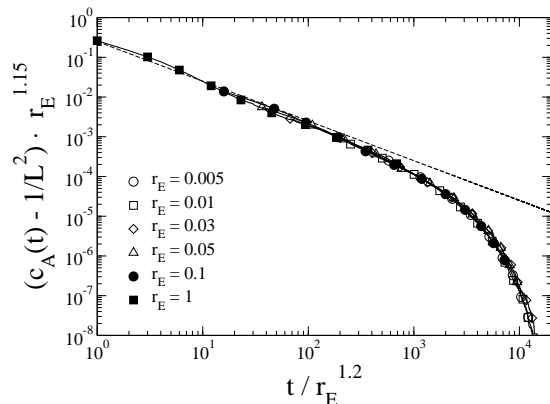


FIG. 5. Scaling of  $c_A(t)$  with  $r_E = E/D$  in  $d = 2$  for  $D/F \rightarrow \infty$ .  $L^2 = 200 \times 200$ .

## VII. SCALING FOR FINITE $D/F$

For finite  $D/F$  there are many  $A$ -clusters on the surface. Their typical distance is given by the diffusion length  $\ell_D$  as shown in Sec.III. The average size of the  $A$ -clusters is  $c_A \ell_D^d$ , provided this is much larger than 1. If the concentration  $c_A$  becomes too small, less and less  $A$ -clusters will be found on the surface, and their typical distance will grow. Finally all  $A$ -atoms will be overgrown, in contrast to the situation of perfect layer-by-layer growth, where the last  $A$ -atom could never be overgrown. Apart

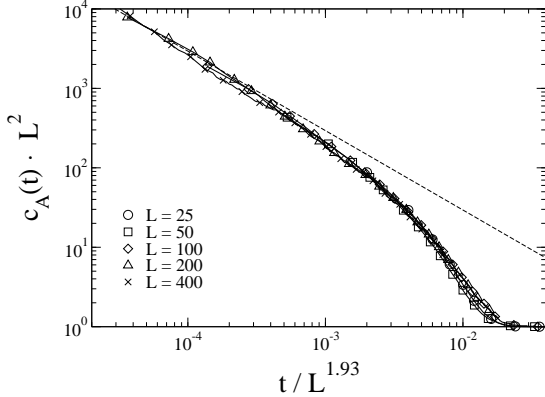


FIG. 6. Scaling of  $c_A(t)$  with  $L$  in  $d = 2$  for  $D/F \rightarrow \infty$ .  $E/D = 0.1$ .

from this, one might expect that the results of the previous three sections would essentially remain true, if one replaces  $L$  by  $\ell_D$ . Qualitatively, the surface concentration  $c_A$  indeed decays first approximately as a power law of the deposition time, which is cut off at a characteristic width  $H$  of the interdiffusion zone.

Quantitatively, however, the situation turns out to be more complex than this: All exponents are different, as the simulation results (Figs. 7 – 10) show. The power law decay of  $c_A \propto t^{-\beta}$  extends over at most two decades for the largest values of  $D/F$  we simulated, so that the determination of the exponent  $\beta$  from the slopes in the log-log-plots Fig.7 and 8 is not very accurate. We estimate

$$\beta = \begin{cases} 0.78 \pm 0.08 & \text{for } d = 1, \\ 0.53 \pm 0.05 & \text{for } d = 2, \end{cases} \quad (16)$$

which are indicated by the dashed lines in the two Figures. Both exponents are significantly smaller than  $\beta = 1$  obtained for infinite  $D/F$ , i.e.  $c_A$  decays more slowly for finite than for infinite  $D/F$ .

This result is surprising on first sight, because there are more island edges on the surface for finite  $D/F$ , hence more possible places, where  $A$ -atoms may be overgrown. That  $c_A$  decays more slowly nevertheless, may be explained by the fact, that the nucleation of islands does not happen anywhere with equal probability as for infinite  $D/F$ , but preferentially far away from the holes in the previous layer, where the  $A$ -atoms are concentrated. Therefore overgrowth is less likely, and  $c_A$  decays more slowly than for infinite  $D/F$ .

This raises the question, how big the parameter  $D/F$  must be in order to see the exponent  $\beta = 1$  instead of the smaller one. The answer is, that the system size  $L$  must be small compared to  $\ell_D$  in order to obtain the crossover to the faster decay of  $c_A$ . This was confirmed by simulation results in [18]. In the four Figures belonging

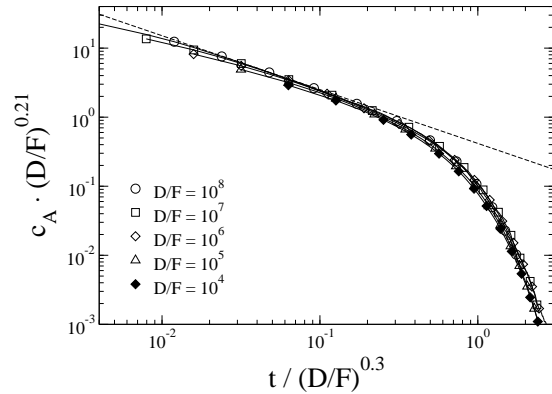


FIG. 7. Scaling of  $c_A(t)$  with  $D/F$  in  $d = 1$ .  $E/D = 10^3, L = 5 \cdot 10^3 \dots 10^4$ . The dashed line indicates the exponent  $\beta = 0.78$ .

to this Section we carefully checked that the system sizes were big enough to exclude finite size effects.

In analogy to Eq.(11) we expect that the power law decay of  $c_A \propto t^{-\beta}$  stops, when

$$r_E(c_A \ell_D^d)^{2/d} \approx 1, \quad (17)$$

or

$$c_A \ell_D^d \approx 1, \quad (18)$$

whichever happens first. Replacing  $c_A$  by  $H^{-\beta}$ , this implies that the width  $H$  of the interdiffusion zone should be given by

$$H \approx \ell_D^{d/\beta} \quad \text{for } r_E \gg 1 \quad (19)$$

and

$$H \approx (\sqrt{r_E} \ell_D)^{d/\beta} \quad \text{for } r_E \ll 1. \quad (20)$$

In analogy to Eq.(13) we postulate then that

$$c_A = \frac{1}{H^\beta} g\left(\frac{t}{H}\right) \quad (21)$$

with

$$g(\tau) \sim 1/\tau^\beta \quad \text{for } \tau \ll 1, \quad (22)$$

because  $c_A$  is independent of  $H$  for small  $t$ .

We first checked these conjectures for  $r_E > 1$ , where the surface concentration of  $A$ 's becomes independent of  $r_E$ , as expected. If we insert the  $D/F$ -dependence Eq.(1) of the diffusion length in Eq.(19), Eq.(21) can be written in the form

$$c_A \left(\frac{D}{F}\right)^{\gamma d} = g_1 \left(t \left(\frac{D}{F}\right)^{-\gamma d/\beta}\right). \quad (23)$$

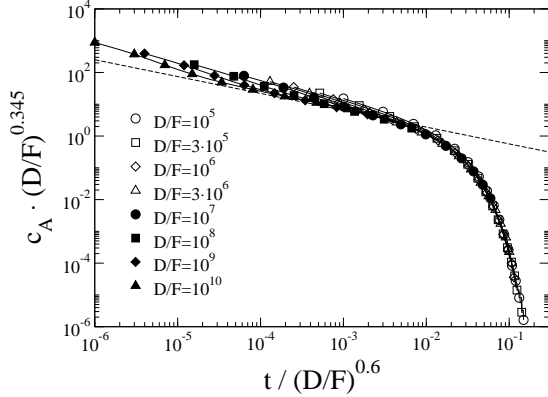


FIG. 8. Scaling of  $c_A(t)$  with  $D/F$  in  $d = 2$ .  $E/D = 10^4$ ,  $L^2 = 500 \times 500$ . The dashed line indicates the exponent  $\beta = 0.53$ .

With  $\gamma = 1/4$  [19] for  $d = 1$  and  $\gamma = 1/(4+d_f) \approx 0.17$  for  $d = 2$  ( $d_f$  is the fractal dimension of the islands) [20], and with the  $\beta$ -values determined above, the theory predicts

$$\gamma d = \begin{cases} 0.25 & \text{for } d = 1 \\ 0.35 \pm 0.01 & \text{for } d = 2 \end{cases} \quad (24)$$

$$\gamma d / \beta = \begin{cases} 0.32 \pm 0.03 & \text{for } d = 1 \\ 0.66 \pm 0.07 & \text{for } d = 2 \end{cases} \quad (25)$$

The data collapses in Figs.7, 8 are in reasonable agreement with this prediction.

However, the  $r_E$ -dependence Eq.(20) for  $r_E < 1$  is not in agreement with the simulation results. For fixed  $D/F$  the theory Eq.(21) predicts

$$c_A r_E^{d/2} = g_2(t r_E^{-d/2\beta}). \quad (26)$$

Inserting the value of  $\beta$  determined above, the scaling exponent should be

$$d/2\beta = \begin{cases} 0.64 \pm 0.06 & \text{for } d = 1 \\ 1.9 \pm 0.2 & \text{for } d = 2 \end{cases} \quad (27)$$

For  $D/F = 10^7$  we could only check this for about one decade of  $r_E$ -values: For  $d = 1$  we found that already for  $r_E = 0.3$  the crossover into the regime, where  $H$  becomes independent of  $r_E$ , affects the data. For  $r_E < 10^{-3}$  the exchange was so weak that the surface concentration of  $A$ 's decayed very fast from the beginning, so that a convincing data collapse was not possible. Similar problems occurred for  $d=2$ . The best result of our attempts to get a data collapse in the available  $r_E$ -interval are shown in Fig.9 for  $d = 1$  and Fig. 10 for  $d = 2$ . The effective exponents turn out to be very different from the ones predicted in Eq.(26).

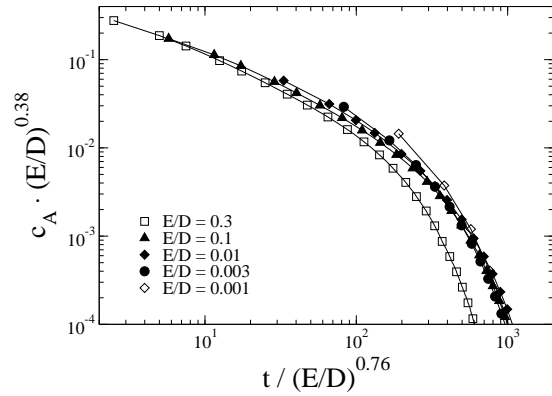


FIG. 9. Scaling of  $c_A(t)$  with  $E/D$  in  $d = 1$ .  $D/F = 10^7$ ,  $L = 5 \cdot 10^3$ .

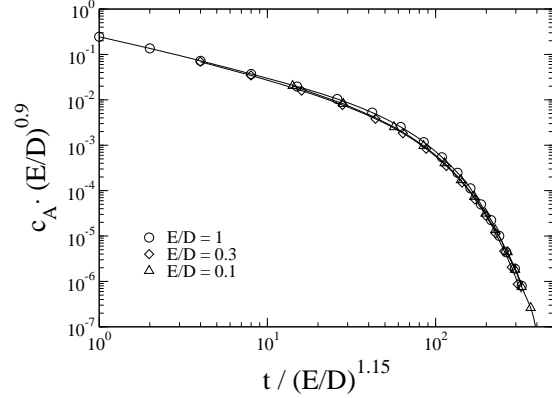


FIG. 10. Scaling of  $c_A(t)$  with  $E/D$  in  $d = 2$ .  $D/F = 10^7$ ,  $L^2 = 500 \times 500$ .

## VIII. RATE EQUATION APPROACH

In this Section we extend the established rate equation approach for submonolayer homoepitaxial growth as described in [21,22], in order to apply it to our model for surface interdiffusion. Our approach describes the time evolution of four submonolayer quantities: The density of mobile adatoms  $\rho$ , the total island density  $I$ , the density of mobile adatoms of type  $B$ ,  $\rho_B$ , and the density of potential exchange partners of type  $A$  in the lower layer,  $\rho_A$ . With these quantities, the rate equations are as follows:

$$\dot{\rho} = F - D\rho(I + 2\rho), \quad (28)$$

$$\dot{I} = D\rho^2, \quad (29)$$

$$\dot{\rho}_B = F - D\rho_B(I + \rho + \rho_B) - Ea^2\rho_A\rho_B, \quad (30)$$

$$\dot{\rho}_A = -Ea^2\rho_A\rho_B - \rho_A a^2 D\rho(I + 2\rho). \quad (31)$$

While the first two equations are identical to the well known point-island model rate equations for homoepitaxial growth, the last two are specific to our heteroepitaxial model. The third one expresses the change in density of the  $B$ -type adatoms. Its positive contribution describes the deposition of new adatoms. The first negative term represents the loss of  $B$ -adatoms, when they get incorporated into islands or bind to another adatom to nucleate a new island. The extra term  $D\rho_B^2$  accounts for the fact that nucleation events involving two  $B$ -adatoms count twice as much as those between a  $B$ - and an  $A$ -adatom, because they remove two  $B$ -adatoms simultaneously. The last term of Eq.(30) describes the exchange of mobile  $B$ 's with  $A$ 's. Equation (31) expresses the annihilation of possible  $A$ -type exchange partners in the lower layer. Since this value is monotonously decreasing, there is no positive contribution. The negative terms describe the exchange of  $A$ 's with mobile  $B$ 's, and the overgrowth of  $A$ 's due to propagating island edges and nucleation events.

Rescaling the variables (see [21]) according to  $\hat{t} = tF\ell_0^2$ ,  $\hat{\rho} = \rho\ell_0^2$ ,  $\hat{I} = I\ell_0^2$ ,  $\hat{\rho}_A = \rho_A\ell_0^2$ ,  $\hat{\rho}_B = \rho_B\ell_0^2$ , where  $\ell_0 = (D/F)^{1/4}$ , leads to the dimensionless equations

$$\dot{\hat{\rho}} = 1 - \hat{\rho}(\hat{I} + 2\hat{\rho}), \quad (32)$$

$$\dot{\hat{I}} = \hat{\rho}^2, \quad (33)$$

$$\dot{\hat{\rho}}_B = 1 - \hat{\rho}_B(\hat{I} + \hat{\rho} + \hat{\rho}_B) - r_E\hat{\rho}_A\hat{\rho}_B, \quad (34)$$

$$\dot{\hat{\rho}}_A = -r_E\hat{\rho}_A\hat{\rho}_B - (a/\ell_0)^2\hat{\rho}_A\hat{\rho}(\hat{I} + 2\hat{\rho}). \quad (35)$$

If we consider systems in perfect layer-by-layer growth mode, this approach not only holds for the submonolayer regime starting from the substrate, but also starting after integer numbers of deposited monolayers. The initial conditions of these equations for a flat surface after  $n$  deposited monolayers are

$$\hat{\rho}(0) = \hat{I}(0) = \hat{\rho}_B(0) = 0, \quad \hat{\rho}_A(0) = \hat{c}_A(n). \quad (36)$$

Disregarding the point island model nature of this approach, which only holds for early stages of the submonolayer regime, we can establish the surface concentration of  $A$ 's after the deposition of one additional monolayer,  $c_A(n+1)$ , as the integral over the density of all exchanged atoms:

$$\hat{c}_A(n+1) = \int_0^{(\ell_0/a)^2} dt r_E \hat{\rho}_A \hat{\rho}_B \quad (37)$$

The upper integration boundary is the dimensionless time for depositing one monolayer. This approximation can be justified by taking into account that the transport of  $A$ -atoms from the  $n$ th to the  $(n+1)$ th layer mainly takes place at early times, that is, the nucleation regime and early stages of the intermediate coverage regime, as explained in section III. The chosen approach describes these regimes with sufficient accuracy.

The solution of the first two equations can be taken directly from the literature [22]: For early times,  $\hat{t} \ll 1$ ,

$\hat{\rho}$  is linear in  $\hat{t}$ , and  $\hat{I}$  increases with  $\hat{t}^3$ . At late times,  $\hat{t} \gg 1$ , one gets  $\hat{\rho} \propto \hat{t}^{1/3}$  and  $\hat{I} \propto \hat{t}^{-1/3}$ .

With these results, the last two equations can be solved analytically in a similar way for the early-time regime,  $\hat{t} \ll 1$ . For equation (34), the second term on the right hand side can be neglected in this limit. If we also neglect the time dependence of  $\hat{\rho}_A(t) \approx \hat{\rho}_A(0) = \hat{c}_A(n)$ , we get

$$\dot{\hat{\rho}}_B \approx 1 - r_E \hat{c}_A \hat{\rho}_B \quad (38)$$

This equation relaxes into a steady state with  $\hat{\rho}_{B,\infty} \propto 1/(r_E \hat{c}_A)$  after a characteristic time  $\hat{t}^* \approx 1/(r_E \hat{c}_A(n))$ . For even smaller times,  $\hat{t} \ll \hat{t}^*$ , we can also neglect the other right hand side term, and we get  $\hat{\rho}_B \propto \hat{t}$ .

Plugging these results into Eq.(35), and realizing that the second term on the right hand side can be neglected compared to the first one, we get

$$\hat{\rho}_A \propto e^{-\hat{t}/\hat{c}_A} \approx \left(1 - \frac{\hat{t}}{\hat{c}_A}\right) \quad \text{for} \quad \hat{t}^* \ll \hat{t} \ll 1 \quad (39)$$

and

$$\hat{\rho}_A \propto e^{-r_E \hat{t}^2} \approx (1 - r_E \hat{t}^2) \quad \text{for} \quad \hat{t} \ll \hat{t}^* \quad (40)$$

To relate these findings to our results in the other sections, we employed an iteration scheme for the rate equation system to obtain the surface concentration of  $A$ 's for every deposited integer monolayer. Starting from the substrate ( $\rho_A(0) = c_A(0) = 1$ ) we can obtain  $\rho_A(1) = c_A(1)$  from Eq.(37) by solving Eqs.(32) – (35) numerically. Plugging  $c_A(1)$  back into our rate equations as the initial surface concentration, that is  $\rho_A(0) = c_A(1)$ , we get  $\rho_A(1) = c_A(2)$  by using Eq.(37) again. Repeating this iteration scheme leads to  $c_A(t)$ .

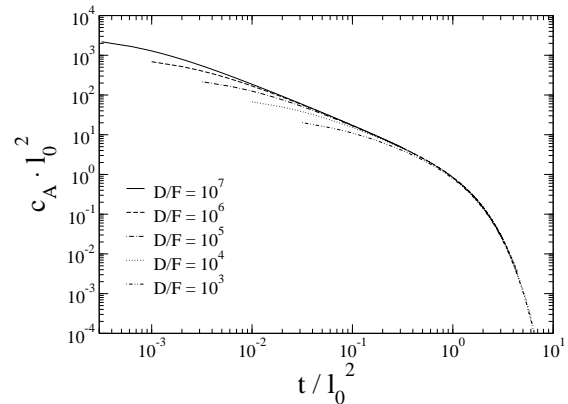


FIG. 11. Scaled time dependence of the surface concentration of substrate atoms, obtained from the iteration of the rate equations. The slope of the power law region is  $-1.03 \pm 0.05$ .  $E/D = 1$ .

The rescaled results of this approach for different  $D/F$  are shown in Fig. 11. One can clearly observe power law



decay for high  $D/F$  values at intermediate times, and a similar scaling behaviour as obtained from the simulations. The exponent of the power law behaviour is approximately  $-1$ , which is identical to the result from the simulations for perfect layer-by-layer growth mode,  $D/F \rightarrow \infty$ . This fact supports our argumentation concerning the different exponents for  $D/F \rightarrow \infty$  and finite  $D/F$  in section VII: Since the rate equations cannot describe the clustering of the  $A$ -atoms, they also do not reflect the preference of the nucleation sites to be far from the  $A$ -clusters. The observed scaling exponent of  $l_0^2 = (D/F)^{1/2}$  doesn't match any of the exponents resulting from the simulations. This is in general agreement with the analytical calculation of the exponents in section V: There we derived the scaling exponents from characteristic properties of the  $A$ -clusters, which are totally neglected in the presented rate equation approach.

## IX. CONCLUSION

In the present work we have investigated heteroepitaxial growth of  $B$ -particles on an  $A$ -substrate. Introducing an exchange mechanism for  $B$ -adatoms, when they encounter an  $A$ -atom in the uppermost layer, we observed that in the limit of layer-by-layer growth the top layer concentration of  $A$ -atoms decays algebraically. Therefore, the resulting interdiffusion zone has a broad profile with a diverging width. Varying the rate  $E$  at which  $A$ -atoms and  $B$ -atoms are exchanged did not change the exponent of this power law. A different situation has been observed, as we varied the diffusion constant  $D$ . For finite values of  $D$  a crossover from power law to exponential decay has been found. The crossover time  $H$  is given by  $(D/F)^{0.3}$  for  $d = 1$  and by  $(D/F)^{0.6}$  for  $d = 2$ .

It would be very interesting to have some experimental results for the concentration of substrate atoms in the growing layer in the case of heteroepitaxy. The results we found suggest that in order to provide a sharp interface between substrate and deposited material one should use small  $D/F$ .

## ACKNOWLEDGMENTS

We are very grateful to H. Hinrichsen, L. Brendel, V. Uzdin, U. Koehler, C. Wolf and A. Lorke, with whom we had many fruitful discussions. This work was supported by the DFG within Sonderforschungsbereich 491 (Magnetic Heterolayers) and GK 277 (Struktur und Dynamik of Heterogeneous Systems), as well as by the INTAS-project 2001-0386. Work done by SBL was supported in part by Korea Research Foundation Grant (KRF-2001-015-DP0120).

## APPENDIX

Here we describe, how we implemented the model introduced in Sec. II for one dimensional surfaces in the limit  $D/F \rightarrow \infty$ . We first describe the idea for the scale free limit, where also  $E/D \rightarrow \infty$ .

For  $D/F \rightarrow \infty$  one has perfect layer-by-layer growth. The nucleation of a new layer happens at an arbitrary position. Afterwards there is at most one adatom on the surface. The idea is to calculate the probabilities exactly, with which the adatom reaches the nearest sinks to its left and to its right. For an  $A$ -adatom these are the island edges, while for a  $B$ -adatom it might also be an  $A$ -atom, with which it could exchange. Let  $d_L$  ( $d_R$ ) denote the distance to the nearest sink to the left (right).

As shown in [23], the probability  $p_L$  to reach the left position prior to the right one with unbiased diffusion is given by

$$p_L = \frac{d_R}{d_R + d_L} \quad (41)$$

Correspondingly,  $p_R = 1 - p_L$ . Therefore, it is not necessary to simulate the whole random walk of an adatom, but it suffices to select the final position according to (41).

Thus in the scale free limit the model (after nucleation of a new layer) may be simulated as follows:

- (1) Deposition of a  $B$  at a randomly chosen site  $i$ .
- (2) Determination of the distances  $d_L$  and  $d_R$  followed by a decision for a side according to the probabilities given in (41).
- (3) If the final position of the  $B$ -adatom is an  $A$ -site, the atoms exchange (as  $E/D \rightarrow \infty$ ). In this case the  $A$ -adatom goes to the left or right island edge according to (41). If the final position of the  $B$ -adatom is an island edge, it is bound there irreversibly possibly overgrowing an  $A$ -atom. Then one returns to step (1) and deposits the next  $B$ -atom.

This algorithm can be generalized for finite  $r_E = E/D$ : Not always, when a  $B$ -adatom encounters an exchange partner  $A$ , they exchange immediately. This happens only with probability  $p_E = E/(E + 2D)$ , where the denominator is the sum of the rates for the three possible actions of the adatom – exchange with the  $A$ -atom underneath, a hop to the right neighbour and a hop to the left neighbour. With probability  $p_E$  the  $B$ -adatom is replaced by an  $A$ -adatom, which attaches to the island edges to its left with probability Eq.(41), and otherwise to the island edge to its right;  $1 - p_E$  is the probability that the  $B$ -adatom continues to diffuse until it encounters the next  $A$ -atom or attaches to the island edge.

In order to avoid simulating the random walk explicitly, one has to calculate the probabilities analytically, that the  $B$ -adatom exchanges with any particular of the  $A$ -atoms or attaches to the island edges. Technically speaking, the  $B$ -atom is a random walker on a one-

dimensional lattice with fixed partial absorbers (the  $A$ -atoms) and two full absorbers (the island edges) (Rosenstock trapping model with partial absorbers). In order to calculate the absorption probabilities at the different absorbers, which depend on the deposition site, we consider an incoming flux (normalized to 1) of independent random walkers at the deposition site  $x_S$  (source) and determine the outgoing fluxes at the absorption sites (sinks). The absorption probability is then the steady state fraction of the incoming flux that leaves the system at the respective absorption site.

The density of random walkers at a site  $x$  evolves according to

$$\dot{\rho}(x, t) = D[\rho(x-1, t) - 2\rho(x, t) + \rho(x+1, t)] - E\rho(x, t)\rho_A(x) + \delta_{x, x_S}, \quad (42)$$

where the density of partial absorbers,  $\rho_A(x)$ , is 1 at all the sites  $x_A$ , where an  $A$ -atom sits, and 0 otherwise:

$$\rho_A(x) = \sum_{\nu=1}^n \delta_{x, x_{A\nu}}. \quad (43)$$

The terms on the right of Eq.(42) which are proportional to  $D$  are the gain and loss terms due to hopping from a neighbor site to  $x$ , respectively away from  $x$ . The term proportional to the exchange rate  $E$  describes the loss of walkers at the partial absorption sites. The last term is the gain term due to the normalized influx of walkers at site  $x_S$ . The perfect sinks corresponding to the island edges are represented by the boundary conditions  $\rho(1) = \rho(L) = 0$ , where  $L$  is the size of the terrace, on which the source is located.

The probability of absorption at site  $x_A$  is then obtained from the steady state solution of Eq.(42) by

$$p(x_A) = E\rho(x_A), \quad (44)$$

and the ones at the island edges by

$$p(1) = D\rho(2), \quad p(L) = D\rho(L-1). \quad (45)$$

Introducing the diffusion current between  $x$  and  $x+1$  (i.e. the current to the right of  $x$  and to the left of  $x+1$ ),

$$j_R(x) = j_L(x+1) = -D(\rho(x+1) - \rho(x)), \quad (46)$$

equation (42) can be rewritten in the steady state as

$$j_R(x) - j_L(x) = -E\rho(x) \sum_{\nu=1}^n \delta_{x, x_{A\nu}} + \delta_{x, x_S}. \quad (47)$$

This shows that  $\rho(x)$  is a piecewise linear function with slope discontinuities at the source and the sinks. Hence Eq.(42) reduces to a set of  $2n+2$  coupled linear equations for the  $2n+2$  unknowns  $j_R(x_{A\nu})$ ,  $\rho(x_{A\nu})$  and the boundary values  $j_R(1)$  and  $j_L(L)$ .

The solution determines the probabilities Eqs.(44), (45) with which a freshly deposited  $B$ -atom is exchanged

at the different  $A$ -sites or absorbed by the island edges. By choosing a random number we decide which site to pick. If it is an island edge, the  $B$ -atom is moved there, and the next  $B$ -atom is deposited at a random position. Otherwise we move the  $B$ -atom to the chosen site, exchange it with the  $A$ -atom there, let another random number determine, whether to attach the  $A$ -atom to the left or right island boundary, and deposit the next  $B$ -atom at a random position.

The complexity of this algorithm is linear in the number of  $A$ -atoms left on the surface, while a brute force simulation of the diffusion would cost much more computing time proportional to  $L^2$ .

- 
- [1] U. Nowak, A. Misra, and K. D. Usadel. Modelling exchange bias microscopically. *J. Magn. Magn. Mat.*, 240:243, 2002.
  - [2] F. S. Bergeret, K. B. Evetov, and A. I. Larkin. Nonhomogeneous magnetic order in superconductor-ferromagnet multilayers. *Phys. Rev. B*, 62:11872, 2000.
  - [3] M. N. Baibich, J. M. Broto, A. Fert, F. NguyenVanDau, F. Petroff, P. Etienne, G. Creuzet, A. Friederich, and J. Chazelas. Giant magnetoresistance of (001)fe/(001)cr magnetic superlattices. *Phys. Rev. Lett.*, 61:2472, 1988.
  - [4] G. Binasch, P. Grünberg, F. Saurenbach, and W. Zinn. Enhanced magnetoresistance in layered magnetic structures with antiferromagnetic interlayer exchange. *Phys. Rev. B*, 39:4828, 1989.
  - [5] F. S. Bergeret, A. F. Volkov, and K. B. Evetov. Enhancement of the josephson critical current by an exchange field in superconductor-ferromagnet structures. *Phys. Rev. Lett.*, 86:3140, 2001.
  - [6] S. A. Wolf, D. D. Awschalom, R.A. Buhrmann, J. M. Daughton, S. von Molnar, M. L. Roukes, A. Y. Chtchelkanova, and D. M. Treger. Spintronics: A spin-based electronics vision for the future. *Science*, 294:1488, 2001.
  - [7] V. M. Uzdin and C. Demangeat. Manipulation of the short-wavelength interlayer exchange coupling in fe/cr multilayers via interface alloying. *Phys. Rev. B* **66**, 0992408, 2002.
  - [8] D. Venus and B. Heinrich. Interfacial mixing of ultrathin cr films grown on an fe whisker. *Phys. Rev. B*, 53:R1733, 1996.
  - [9] M. Krishnamurthy, A. Lorke, and P. M. Petroff. Self-organized lateral superlattice formation by vertical exchange reactions. *Surf. Sci. Lett.* **304**, L493, 1994.
  - [10] C. Wolf and U. Köhler. Intermixing at the interface of the system nb/fe(110) studied with stm. *Surf. Sci. Lett.*, 2003.
  - [11] M. M. J. Bischoff, T. Yamada, A. J. Quinn, R. G. P. van der Kraan, and H. van Kempen. Direct observation of surface alloying and interface roughening: Growth of au on fe(001). *Phys. Rev. Lett.* **87**, 246102-1, 2001.

- [12] K. Schroeder, R. Berger A. Antons, and S. Bluegel. Surfactant mediated heteroepitaxy: Kinetics for group-iv adatoms on as-passivated si(111) and ge(111). *Phys. Rev. Lett.* **88**, 46101, 2002.
- [13] G. L. Kellogg. Field ion microscope studies of single-atom surface diffusion and cluster nucleation on metal surfaces. *Surf. Sci. Rep.*, 21:1, 1994.
- [14] A. C. Levi and M. Kotrla. Theory and simulation of crystal growth. *J. Phys. Cond. Matter*, 9:299, 1997.
- [15] K. Binder, editor. *Monte Carlo Methods in Statistical Physics*. Springer, second edition, 1986.
- [16] M. E. J. Newman and G. T. Barkema. *Monte Carlo Methods in Statistical Physics*. Oxford University Press, 1999.
- [17] M. Kotrla, J. Krug, and P. Smilauer. Submonolayer epitaxy with impurities: Kinetic monte carlo simulations and rate-equation analysis. *Phys. Rev. B* **62**, 2889, 2000.
- [18] B. Bierwald. Zur interdiffusion bei heteroepitaktischem schichtwachstum. *Diplom-Thesis, Gerhard-Mercator-University Duisburg*, 2002.
- [19] A. Pimpinelli, J. Villain, and D. E. Wolf. Surface diffusion and island density. *Phys. Rev. Lett.*, 69:985, 1992.
- [20] J. Villain, A. Pimpinelli, and D. E. Wolf. Layer by layer growth in molecular beam epitaxy. *Comments Cond. Mat. Phys.*, 16:1, 1992.
- [21] L. H. Tang. Island formation in submonolayer epitaxy. *J. Phys. France I* **3**, 935, 1993.
- [22] J. G. Amar, F. Family, and P.-M. Lam. Dynamic scaling of the island size distribution and percolation in a model of submonolayer molecular-beam epitaxy. *Phys. Rev. B* **50**, 8781, 1994.
- [23] C. W. Gardiner. *Handbook of Stochastic Methods*. Springer, 2nd edition edition, 1985.